Crystallinity in Cross-Linked Porous Polymers from High Internal Phase Emulsions

Shulamit Livshin and Michael S. Silverstein*

Department of Materials Engineering, Technion-Israel Institute of Technology, Haifa 32000, Israel

Received May 10, 2007; Revised Manuscript Received June 18, 2007

ABSTRACT: PolyHIPE are cross-linked, highly interconnected porous polymers with unique multiscale, open-pore structures that are based on high internal phase emulsions (HIPE). This work is the first to describe crystallinity in polyHIPE. This novel crystallinity was achieved by using monomers with *n*-alkyl side chains (acrylates and methacrylates). Such crystallinity in polyHIPE could potentially be used to produce porous shape-memory polymers. The higher the molecular mobility and the higher the molecular order (homopolymer vs copolymer, non-cross-linked vs cross-linked, acrylate vs methacrylate, long side chains vs short side chains), the higher the melting point (T_m) and the higher the crystallinity. Only the polyHIPE based on an acrylate with a relatively long (C_{18}) side chain exhibited a significant proportion of its melting peak above room temperature and exhibited a significant heat of melting.

Introduction

A high internal phase emulsion (HIPE) is an emulsion in which the internal phase occupies more than 74% of the volume. PolyHIPE are highly cross-linked porous polymers based on HIPE. PolyHIPE are synthesized by polymerizing monomers and cross-linking comonomers in the HIPE's continuous phase.[1−6] Porous materials have numerous applications in such areas as catalysis, chromatography, and separation, where control over pore structure and pore size strongly influences the efficiency of the material.[7] PolyHIPE, with their high porosities, high degrees of interconnectivity, and unique micrometer to nanometer-scale open-pore structures, are of interest for such applications.[4,8]

PolyHIPE have been synthesized from a wide variety of organic monomers and cross-linking comonomers, and some polyHIPE have included organosilicon components.[1,9−11] Most of these monomers yield amorphous homopolymers. Even monomers which can yield crystalline homopolymers are not likely to yield crystalline polyHIPE owing to the significant amounts of cross-linking comonomers. The cross-linking comonomer disrupts the regularity of the molecular structure along the polymer backbone and restricts polymer mobility, limiting the ability of the backbone to organize into an ordered crystalline structure. However, it might be possible to produce crystallinity within a polyHIPE by using monomers bearing long aliphatic or rigid-rod side chains. The crystalline transition in the polyHIPE could potentially be used to produce highly porous polymers with shape-memory behavior. A shape "locked in" on quenching below the melting point (T_m) would be "unlocked" above the T_m.

Polymers synthesized from monomers bearing long (in most cases aliphatic) side chains form crystalline structures which are somewhat unusual. In conventional semicrystalline polymers, the relatively mobile backbone folds into a crystalline structure. In general, the molecular structures of the crystalline and amorphous phases are identical. Here, the polymer backbone is relatively stiff, owing to the presence of the side chains.[12,13] The side chain flexibility, on the other hand, increases with increasing side chain length. Beyond a minimal length, the side chains become flexible enough to overcome the constraints imposed by the relatively stiff polymer backbone and, in regions far from the polymer backbone, are able to crystallize.[12,14,15] The side chains form paraffin-like hexagonal crystal lattices with Bragg *d*-spacings of around 4.2 Å.[14] The polymer backbone folds into a helical structure.[16] The section of the side chain closest to the backbone is unable to crystallize and remains amorphous. In such comblike polymers, the molecular structures of the crystalline and amorphous phases can be quite different.

The crystalline structure and properties of these polymers can be modified through variations in the backbone and/or through variations in the side chains. The thermal properties (T_m, and heat of fusion, ΔH_f) can be modified by varying the side-chain length. Larger crystallites and narrower size distributions result from increasing the side-chain length and yield increases in T_m and ΔH_f. The minimal length of a C_nH_{2n+1} side chain for side-chain crystallization is dependent on polymer backbone flexibility. When the polymer backbone is more rigid, crystallization requires a longer side chain. The polymer backbone is more rigid for methacrylates than for acrylates, reflecting the additional steric hindrance from the extra methyl group. For poly(*n*-alkyl acrylates), C_9 is the minimal side chain length for crystallization.[14,17,18] For poly(*n*-alkyl methacrylates), C_{12} is the minimal side-chain length.

In general, the crystalline structures and thermal properties of copolymers that include side-chain monomers are similar to those of the homopolymers from those side-chain monomers. Obviously, the presence of monomers that do not have crystallizable side chains disrupts organization of the side chains and impedes crystallization. As a result, the copolymer T_m and crystallinities (X_c) are lower than those of the homopolymer.[19−21] The addition of a cross-linking comonomer will further disrupt organization of the side chains and further impede crystallization, producing lower T_m and X_c.

This work is the first to describe a highly cross-linked polyHIPE with a significant amount of crystallinity. The synthesis and characterization of polyHIPE based on acrylates and methacrylates with *n*-alkyl side chains are described in detail. The influences of the polymer backbone's molecular structure and of the side chain's length on the crystallinity and properties are discussed.

* Corresponding author. E-mail: michaels@tx.technion.ac.il.

10.1021/ma071055p CCC: $37.00
Published on Web 07/24/2007

Table 1. Typical Synthesis Recipe (A12 PolyHIPE)

	component	amount, wt %
organic phase	A12	7.79
	DVB	1.95
	SMO	1.95
aqueous phase	H_2O	87.63
	$K_2S_2O_8$	0.19
	K_2SO_4	0.49

Experimental Section

Materials. The monomers used for polyHIPE synthesis were lauryl acrylate (A12, $CH_2{=}CHCO_2C_{12}H_{25}$, Sigma-Aldrich), lauryl methacrylate (M12, $CH_2{=}C(CH_3)CO_2C_{12}H_{25}$, Fluka Chemie), stearyl acrylate (A18, $H_2C{=}CHCO_2C_{18}H_{37}$, Sigma-Aldrich), and stearyl methacrylate (M18, $H_2C{=}C(CH_3)CO_2C_{18}H_{37}$, Sigma-Aldrich). Divinylbenzene containing 40% ethylstyrene (DVB, Riedel-de-Haen) was the cross-linking comonomer. The inhibitors in A12, M12, M18, and DVB were removed through extraction with 1.25 M NaOH. A18 was used as received. For polyHIPE synthesis, the emulsifier was sorbitan monooleate (SMO, Span 80, Fluka Chemie), the water-soluble initiator was potassium persulfate ($K_2S_2O_8$, Riedel-de-Haen), and the stabilizer was potassium sulfate (K_2SO_4, Frutarom, Israel). The organic phase soluble initiator used for bulk polymerization was benzoyl peroxide (BPO, Fluka Chemie).

PolyHIPE Synthesis. The HIPE was formed by adding the aqueous phase (water, initiator, and stabilizers, about 90% of the total volume) dropwise to the organic phase (monomers and emulsifier, about 10% of the total volume). A typical recipe used for polyHIPE synthesis is listed in Table 1. The mass ratio of 4 parts side-chain monomer (acrylate or methacrylate) and 1 part DVB was used for all the polyHIPE. The corresponding molar contents of DVB are listed in Table 2. The detailed procedure for polyHIPE synthesis was as follows: the organic phase was placed in a beaker and stirred with a magnetic stirrer. Since the T_m of A18 is 34 °C, the organic phase was heated to 40 °C before the aqueous phase was added.

The aqueous phase was added dropwise with constant stirring, and the resulting HIPE was covered with Parafilm. Polymerization took place in a circulating air oven at 65 °C for 18 h. The water was removed from the polyHIPE by drying at room temperature in a vacuum oven for about 3 days, until a constant weight was reached. The surfactant, initiator, and stabilizer, which remain in the polyHIPE following drying, were removed by Soxhlet extraction (water for 24 h and methanol for 24 h). The polyHIPE was then dried in a vacuum oven at room temperature for 24 h.

Bulk Polymerization. Bulk polymerization was used to synthesize control materials. Two types of controls were synthesized: homopolymers (HP) of the side-chain monomers and copolymers (CP) of the side-chain monomer with DVB using the same monomer/DVB ratios used in the polyHIPE. The side-chain monomer, cross-linking comonomer (if applicable), and initiator were mixed in a beaker with a magnetic stirrer. Polymerization took place in a circulating air oven at 65 °C for 18 h. Since the T_m of A18 is 34 °C, the monomer was heated to 40 °C before adding the other components. The initiator (BPO) content was 2 wt % of the monomer content.

Characterization. The density, ρ, was determined by measuring the mass and volume of a specimen. The specific surface area, A, was determined using the single-point BET (Brunauer, Emmett, Teller) method, with nitrogen adsorption−desorption at 77 K (Flowsorb II, Micromeritics). The porous structures of cryogenic facture surfaces were investigated using high-resolution scanning electron microscopy (HRSEM, Zeiss LEO 982). The samples, viewed using an accelerating voltage of 4 kV, were not coated. The crystalline structure was investigated by using X-ray diffraction (XRD, Philips PW 1840 X-ray) with a Ni-filtered Cu Kα X-ray beam excited at 40 kV and 40 mA. The thermal properties (T_m and the heat of the melting endotherm, ΔH) were investigated using differential scanning calorimetry (DSC, Mettler DSC-821 calorimeter). The samples were heated from −100 to 100 °C at a rate of 10 °C/min in nitrogen. The dynamic mechanical properties as a function of temperature were investigated using dynamic mechanical thermal analysis (DMTA, Rheometrics MKIII). The samples were subjected to a sinusoidal compressive strain at a frequency of 1 Hz while heated at a rate of 3 °C/min. The static compressive moduli, E, were determined from the initial slopes of compressive stress−strain curves at room temperature (Rheometrics MKIII). The stress−strain measurements were carried out until equipment-related force or displacement limitations were reached.

Table 2. Compositions, Densities, Specific Surface Areas, and Moduli of the PolyHIPE

	DVB, mol %	ρ, g/cm^3	A, g/m^2	E, MPa
M12	33	0.11	3.5	1.8
A12	32	0.12	2.7	0.5
M18	39	0.11	4.0	1.3
A18	38	0.11	1.3	1.6

Results and Discussion

Porous Structure. The polyHIPE polymerization yields were all above 90%. The densities of the polyHIPE were between 0.11 and 0.12 g/cm^3 (Table 2), as expected from the comonomer to aqueous phase volume ratio. The porosities of the polyHIPE, estimated by assuming a polymer density of 1 g/cm^3, were around 89%. The specific surface areas were typical of polyHIPE, between 2.7 and 4.0 g/m^2 for M12, A12, and M18 (Table 2). The surface area of A18, 1.4 g/m^2, was somewhat smaller than those of the other polyHIPE. The porous structures of the polyHIPE are similar, as seen in Figure 1. There are voids, usually between 10 and 30 μm, that reflect the size of the water droplets in the HIPE. There are also holes, usually between 0.2 and 5 μm. These holes develop within the organic envelope surrounding the water droplets during polymerization. The porous structures for A12 and M12 are quite similar, with the voids and holes being somewhat larger for M12. The holes are somewhat larger for A18 and are significantly smaller for M18. These differences in the porous structure do not seem to be directly related to the nature of the monomer (acrylate or methacrylate), the degree of cross-linking (molar content of DVB), the length of the side chain, or the crystallinity (as discussed below).

Crystalline Structure. There are no crystalline peaks in the X-ray scattering from the A12 polyHIPE, only an amorphous halo (Figure 2). The amorphous halo has a maximum at $2\theta = 18.5°$ that corresponds to a distance of 4.65 Å, the average distance between disordered (amorphous) alkyl chains. X-ray scattering from M12 and M18 yields amorphous halos that are similar to that from A12.

The crystalline reflection protruding from the amorphous halo in the X-ray scattering from A18 (Figure 2) is exceptional. There are no previous reports of significant crystallinity within polyHIPE. The small crystalline reflection at $2\theta = 21.0°$ corresponds to a Bragg d-spacing of 4.20 Å. This Bragg d-spacing is typical of the paraffin-like hexagonal lattice formed by the packing of aliphatic side chains attached to polyacrylates and polymethacrylates.[14] For comparison, the A18 homopolymer has an X-ray reflection at $2\theta = 21.4°$ that corresponds to a Bragg d-spacing of 4.15 Å (Figure 2).

Thermal and Mechanical Properties. T_m and ΔH_f for the monomers are listed in Table 3 and Table 4, respectively.[22,23] The peak temperatures from the DSC thermograms from the HP (not shown), CP (not shown), and polyHIPE (Figure 3) are summarized in Table 3. Estimates for X_c were calculated by dividing ΔH by the number of carbons in the aliphatic side chain and by the ΔH_f of 3.4 kJ/mol per side chain carbon.[18] This estimate for the side chain ΔH_f of the polymers yields results

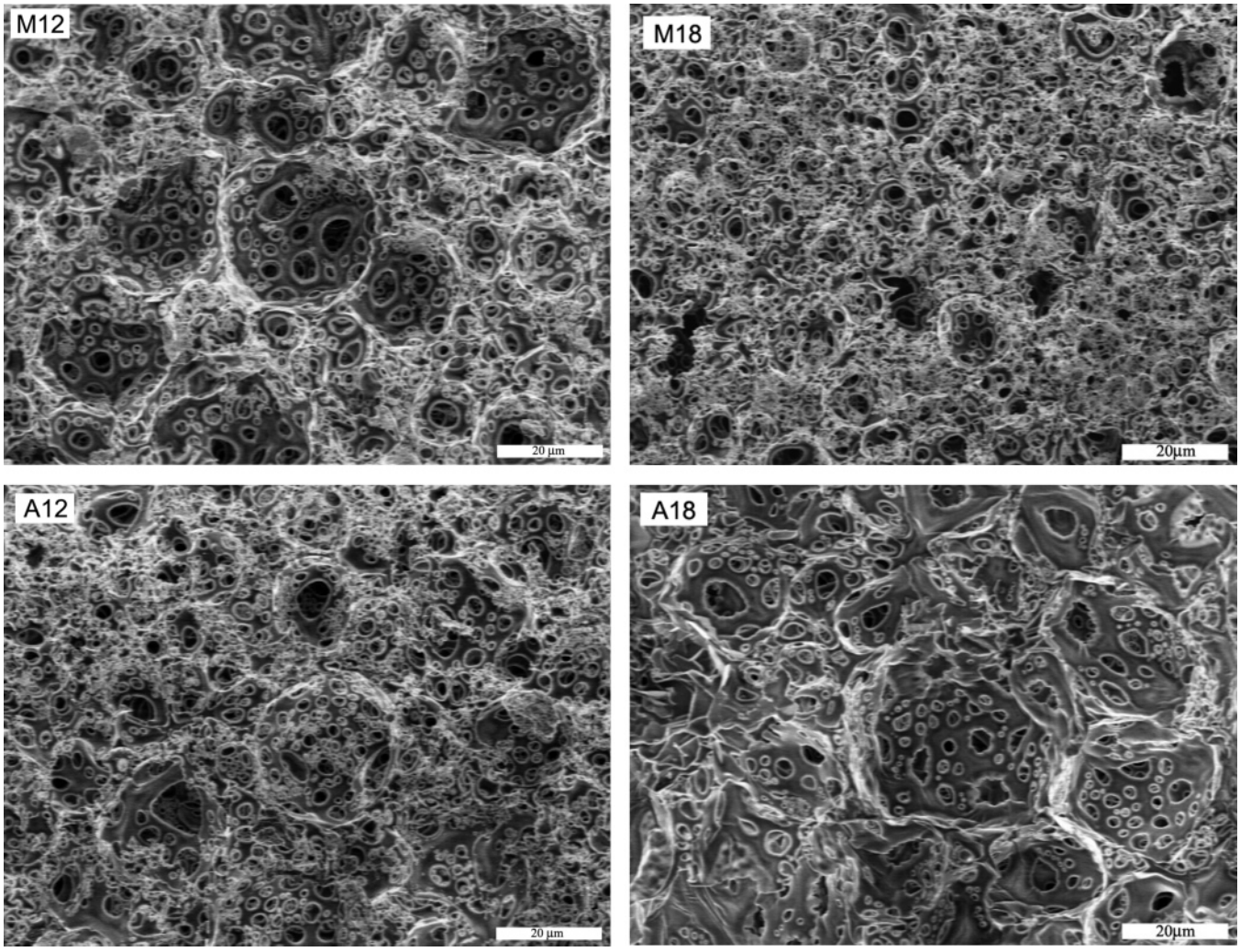

Figure 1. Cryogenic fracture surfaces of the polyHIPE (HRSEM micrographs).

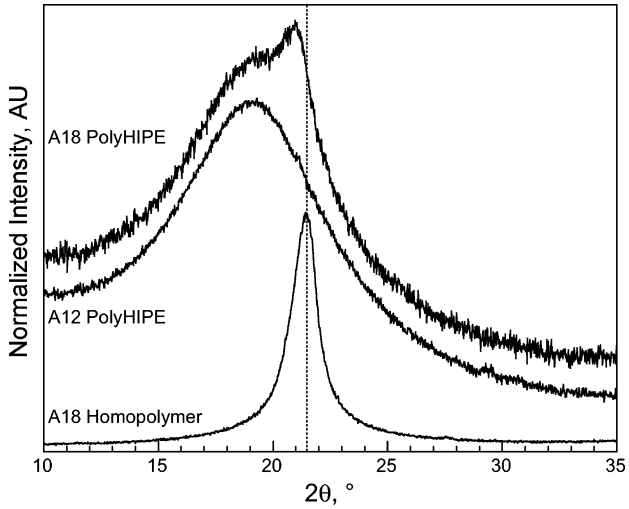

Figure 2. X-ray scattering from the A18 HP, the A18 polyHIPE, and the A12 polyHIPE.

that are quite close to the monomer ΔH_f in Table 4. The heats and crystallinities from the thermograms in Figure 3 are summarized in Table 4. The ordered structure in a cross-linked copolymer with side-chain monomers is illustrated schematically in Table 4. The limitations on crystallization imposed by comonomer content, cross-linking, side chain length, and backbone flexibility can be understood through the effects of these factors on the structure in Figure 4.

Table 3. Monomer T_m;[22,23] DSC and DMTA Peak Temperatures for the HP, CP, and PolyHIPE

	T_m, °C monomer	DSC peaks, °C			tan δ peaks, °C
		HP	CP	polyHIPE	polyHIPE
M12	−7.0	−31.1	−45.7	−46.2	7
A12	1.9	−3.3	−29.7	−9.4	−11
				(15.9)	(18)
M18	19.0	34.8	2.1	−8.9	13
			(23.0)	(32.4)	
A18	33.9	48.4	22.6	19.0	18
				43.8	
			(57.0)	(58.6)	(53)

Table 4. Monomer ΔH_f;[22] DSC Endotherm Peak Areas and Crystallinities for the HP, CP, and PolyHIPE

	ΔH_f, kJ/mol monomer	ΔH, kJ/mol (X_c, %)		
		HP	CP	polyHIPE
M12		−10.6 (26)	−1.0 (3)	−1.2 (3)
A12	42.5	−19.7 (48)	−4.2 (10)	−2.6 (6)
M18		−34.4 (56)	−10.5 (17)	−6.6 (11)
A18	62.2	−44.8 (73)	−14.3 (23)	−20.0 (33)

For the HP and CP, the melting peak temperatures of the polymers with C_{18} side chains are 50−60 °C higher than those of the polymers with C_{12} side chains, reflecting their ability to pack into structures with higher degrees of order.[17] For both the HP and CP, the peak temperatures of the methacrylates are 15−30 °C lower than those of the acrylates, reflecting the more limited flexibilities of their backbones. The CP peak tempera-

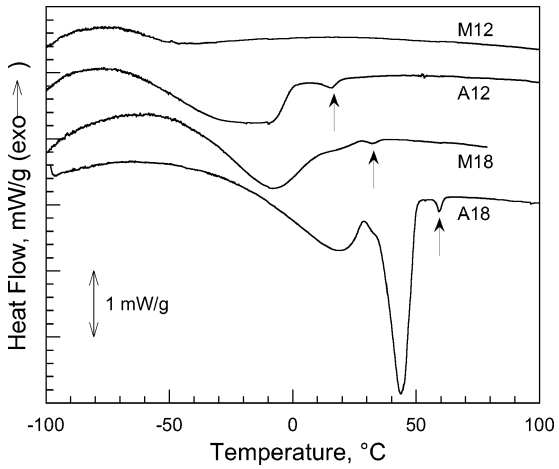

Figure 3. PolyHIPE thermograms (DSC).

tures are 15−30 °C lower than those of the HP, reflecting the limitations on crystalline packing imposed by copolymerization and cross-linking.

All four polyHIPE exhibit melting endotherms in Figure 3. The thermograms for the methacrylate polyHIPE are quite similar to the thermograms of the copolymers and, in general, the T_m are similar. The thermograms for the acrylate polyHIPE incorporate features found in both the homopolymer and copolymer thermograms. The A18 homopolymer and copolymer peaks are relatively large and distinct. The A18 polyHIPE exhibits one peak at 19.0 °C which corresponds to the copolymer (22.6 °C) and a second, larger, peak at 43.8 °C which corresponds to the homopolymer (48.4 °C). The A12 homopolymer and copolymer peaks are smaller, broader, and overlap more considerably. The main peak for the A12 polyHIPE corresponds to the homopolymer peak. The shoulder at −30 °C for the A12 polyHIPE corresponds to the copolymer (−29.7 °C).

The polyHIPE exhibit the same trends as described above with respect to the effects of side-chain length, acrylate vs methacrylate, and cross-linked copolymers vs homopolymers. M12 exhibits the smallest endotherm, and A18 exhibits an endotherm that is significantly larger than those of the other polyHIPE. The peak temperatures for the M12, A12, and M18 polyHIPE in Table 3 are all below room temperature. Therefore, only the A18 polyHIPE can be expected to exhibit crystalline reflections at room temperature, confirming the XRD results.

Interestingly, both the CP and the polyHIPE exhibit small endothermic peaks anywhere from 10 to 40 °C above the main endothermic peak (marked with arrows in Figure 3, in parentheses in Table 3). These peaks seem to be more prominent in the acrylates than in the methacrylates and more prominent for the longer side chains. These relatively high temperature peaks, not seen in the HP, are associated with DVB copolymerization. The A18 polyHIPE has a such a peak at 58.6 °C, and the A18 CP has a similar peak at 57.0 °C. The presence of these peaks may indicate that there exists a compositional distribution on the nanometer scale, with DVB-rich areas and DVB-poor areas.

The ΔH for the polyHIPE are similar to those for the CP, and both are significantly smaller than those for the HP. The dependence of ΔH on the molecular structure of the backbone and on the side-chain length are the same as observed for the HP. ΔH increases with side-chain length, and ΔH is higher for acrylates than for methacrylates. The polyHIPE crystallinity for M12 is 3% and for A18 is 33%. The crystallinity consistently increases in the order M12, A12, M18, and A18 for the HP, CP, and polyHIPE. The more mobile the backbone and the more mobile the side chain, the higher the crystallinity. The ratios of polyHIPE crystallinity to HP crystallinity for M12, A12, M18, and A18 are 0.12, 0.13, 0.20, and 0.45, respectively. As the backbone flexibility increases and as the length of the side chain increases, the polyHIPE is not only able to achieve a higher crystallinity, but the crystallinity is also more similar to the crystallinity of the corresponding HP.

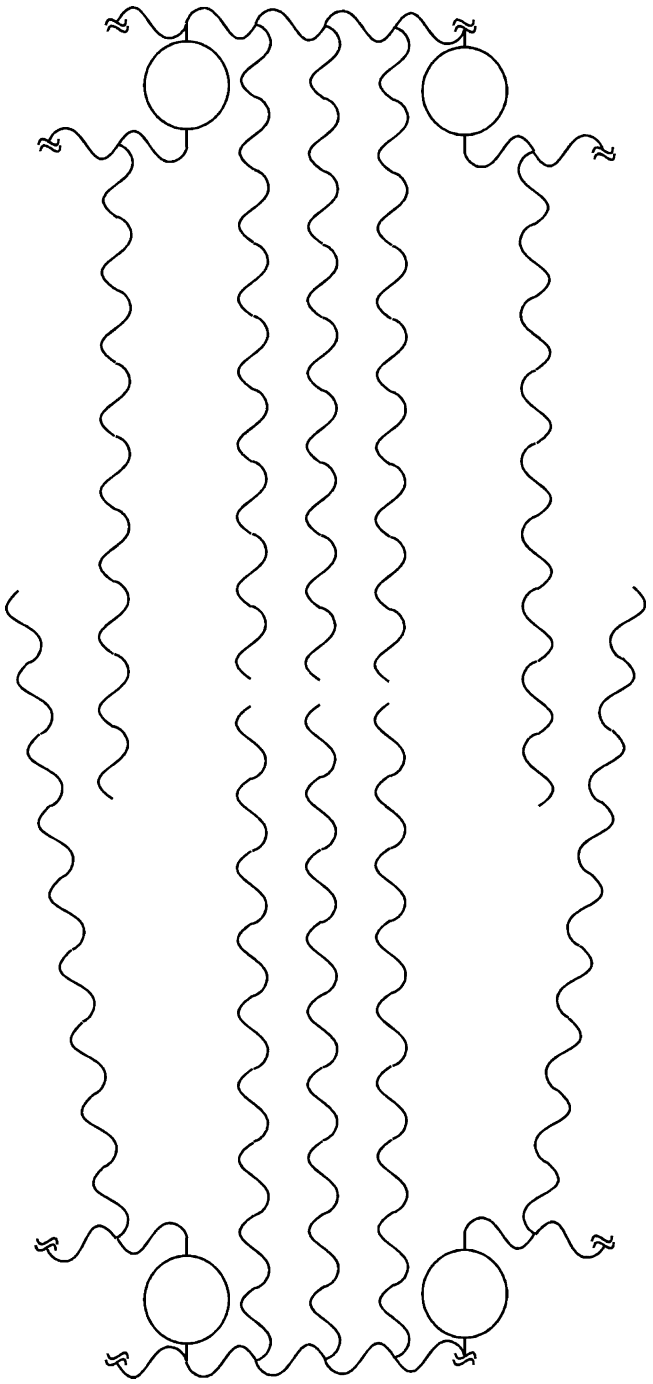

Figure 4. Schematic illustration of crystalline ordered structure in a cross-linked copolymer with side chain monomers.

The variations in the polyHIPE E' and tan δ with temperature are seen in Figure 5 and Figure 6, respectively. The curves in Figures 5 and 6 were shifted vertically to enhance clarity. The E' plateaus at low temperatures are similar for most of the polyHIPE (an E' at −80 °C of around 11 MPa for M12, A12, and M18). A18 exhibits a somewhat lower E' plateau (an E' at −80 °C of 4.5 MPa). E' decreases by 2 orders of magnitude with increasing temperature (Figure 5). The E' plateaus at high

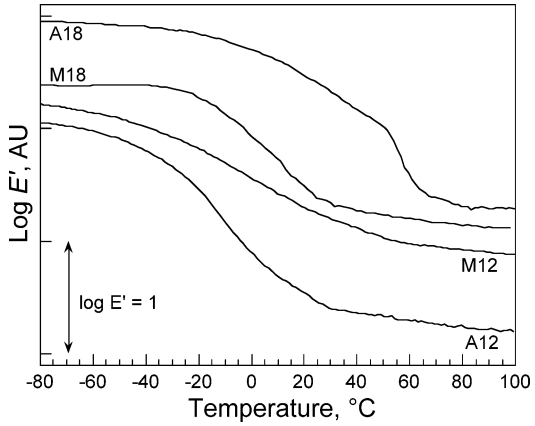

Figure 5. Variation of polyHIPE E' with temperature (DMTA). The curves have been shifted vertically for clarity.

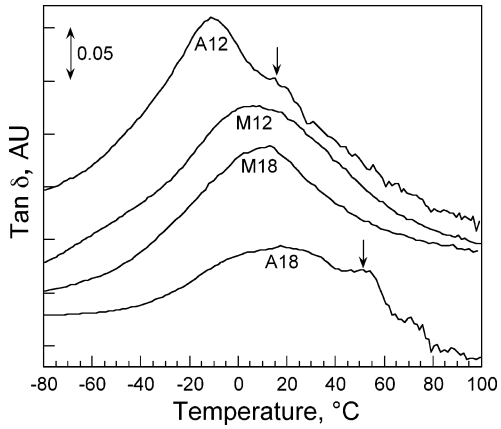

Figure 6. Variation of polyHIPE tan δ with temperature (DMTA). The curves have been shifted vertically for clarity.

temperatures are somewhat higher for the methacrylates than for the acrylates (an E' at 90 °C of around 0.6 and 0.1 MPa for the methacrylates and acrylates, respectively), reflecting the greater rigidity of the methacrylate backbone.

The transitions from rigid materials (E' plateau at low temperatures) to flexible materials (E' plateau at high temperatures) are unusually broad. Such broad transitions have been reported for the glass transition temperatures (T_g) in polyHIPE and in interpenetrating polymer networks (IPN). The large breadths of such transitions can reflect limitations on molecular mobility imposed by the high degree of cross-linking and/or a compositional distribution on the nanometer scale.[4,9,10,24−28] In general, the tan δ peak temperatures in Table 3 are quite similar to the corresponding DSC endotherm peak temperatures. The maximum tan δ values vary from 0.11 for A18 to 0.21 for A12.

Interestingly, there are shoulders in the tan δ peaks for A12 and A18 (marked with arrows in Figure 6, in parentheses in Table 3) that correspond to the small endothermal peaks seen at relatively high temperatures in Figure 3. Here again, the transition is more pronounced for the more mobile acrylates than for the less mobile methacrylates and is more pronounced for the longer, more mobile side chains. This seems to confirm that DVB copolymerization yields a distinct transition whose prominence seems to depend on the molecular mobility and which can affect the properties.

All four polyHIPE exhibit typical stress−strain curves in Figure 7. There is a steep increase in stress at low strains, then a stress plateau, and then another steep increase in stress. The polyHIPE moduli range between 0.5 and 1.6 MPa (Table 2). The modulus and stress plateau are highest for M12 and lowest

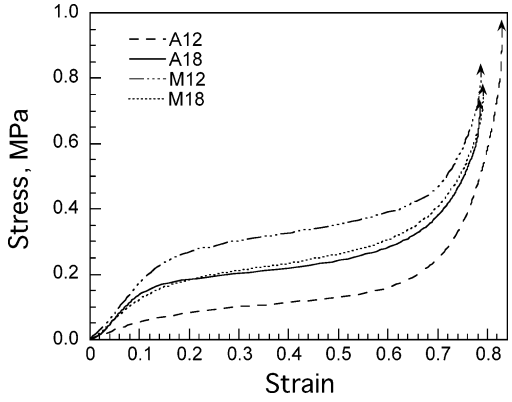

Figure 7. PolyHIPE compressive stress−strain curves.

for A12. The moduli and stress plateaus are similar for A18 and M18. There seems to be no direct relationship between the mechanical behavior and the porous structure, the molecular structure of the backbone, the degree of cross-linking, or the side-chain length.

Conclusions

Novel polyHIPE containing crystalline *n*-alkyl side chains with acrylate and methacrylate backbones were successfully synthesized. The densities (around 0.11 g/cm^3) and the porous structures (voids on the order of 20 μm and holes on the order of 1 μm) are typical of polyHIPE. All the polyHIPE exhibit melting peaks, but only the A18 polyHIPE exhibited a significant proportion of its melting peak above room temperature and exhibited a significant heat of melting. The crystalline phase in the A18 polyHIPE has a Bragg *d*-spacing of 4.20 Å, typical of side-chain paraffin-like hexagonal lattices. In general, the polyHIPE melting peak temperatures and heats of melting are more similar to those of the corresponding CP and are significantly lower than those of the corresponding HP, reflecting the disruption of the ordered structure on copolymerization/cross-linking. The melting peak temperatures and the crystallinities are higher for the acrylate backbones and for the longer side chains, both of which enhance the mobility. A small transition at relatively high temperatures, associated with DVB cross-linking, is more prominent for the more mobile polymers. The polyHIPE's unusually broad tan δ peaks can be associated with highly cross-linked structures and/or a compositional distribution on the nanometer scale.

Acknowledgment. The partial support of the Technion VPR fund is gratefully acknowledged.

References and Notes

(1) Cameron, N. R.; Sherrington, D. C. *J. Mater. Chem.* **1997**, *7*, 2209.
(2) Cameron, N. R. *Polymer* **2005**, *46*, 1439.
(3) Sergienko, A. Y.; Tai, H.; Narkis, M.; Silverstein, M. S. *J. Appl. Polym. Sci.* **2004**, *94*, 2233.
(4) Tai, H.; Sergienko, A.; Silverstein, M. S. *Polym. Eng. Sci.* **2001**, *41*, 1540.
(5) Sergienko, A. Y.; Tai, H.; Narkis, M.; Silverstein, M. S. *J. Appl. Polym. Sci.* **2002**, *84*, 2018.
(6) Mezzenga, R.; Ruokolainen, J.; Fredrickson, G. H.; Kramer, E. J. *Macromolecules* **2003**, *36*, 4466.
(7) Zhang, H.; Hardy, G. C.; Khimyak, Y. Z.; Rosseinsky, M. J.; Cooper, A. I. *Chem. Mater.* **2004**, *16*, 4245.
(8) Busby, W.; Cameron, N. R.; Jahoda, C. A. B. *Biomacromolecules* **2001**, *2*, 154.
(9) Silverstein, M. S.; Tai, H. W.; Sergienko, A.; Lumelsky, Y. L.; Pavlovsky, S. *Polymer* **2005**, *46*, 6682.
(10) Tai, H.; Sergienko, A.; Silverstein, M. S. *Polymer* **2001**, *42*, 4473.

(11) Normatov, J.; Silverstein, M. S. Porous Polymer-POSS Nanocomposites Synthesized within High Internal Phase Emulsions, submitted for publication.
(12) Zanuy, D.; Zazueta, D. A.; Aleman, C. *Polymer* **2003**, *44*, 4735.
(13) Curco, D.; Aleman, C. *J. Polym. Sci., Part B: Polym. Phys.* **2006**, *44*, 953.
(14) Plate, N. A.; Shibaeve, V. P. *J. Polym. Sci., Macromol. Rev.* **1974**, *8*, 117.
(15) Jordan, E. F. *J. Polym. Sci., Part A1: Polym. Chem.* **1972**, *10*, 3347.
(16) Hempel, E.; Budde, H.; Horing, S.; Beiner, M. *J. Non-Cryst. Solids* **2006**, *352*, 5013.
(17) Jordan, E. F.; Feldeise, D. W.; Wrigley, A. N. *J. Polym. Sci., Part A1: Polym. Chem.* **1971**, *9*, 1835.
(18) Hempel, E.; Huth, H.; Beiner, M. *Thermochim. Acta* **2003**, *403*, 105.
(19) Jordan, E. F.; Arthymys. R.; Speca, A.; Wrigley, A. N. *J. Polym. Sci., Part A1: Polym. Chem.* **1971**, *9*, 3349.
(20) O'Leary, K. A.; Paul, D. R. *Polymer* **2006**, *47*, 1226.
(21) O'Leary, K. A.; Paul, D. R. *Polymer* **2006**, *47*, 1245.
(22) Edmund, F. J., Jr. *J. Polym. Sci., Part A1: Polym. Chem.* **1972**, *10*, 3347.
(23) Bloch, D. R. In *Polymer Handbook*, 4th ed.; Brandrup, J., Immergut, E. H., Grulke, E. A., Eds.; John Wiley and Sons: New York, 1999; pp III/8−II/16.
(24) Silverstein, M. S.; Narkis, M. *J. Appl. Polym. Sci.* **1990**, *40*, 1583.
(25) Silverstein, M. S.; Narkis, M. *Polym. Eng. Sci.* **1989**, *29*, 824.
(26) Silverstein, M. S.; Narkis, M. *J. Appl. Polym. Sci.* **1987**, *33*, 2529.
(27) Thomas, D. A.; Sperling, L. H. In *Polymer Blends*; Paul, D. R., Newman, S., Eds.; Academic Press: New York, 1978; Vol. 2, pp 20−29.
(28) Sperling, L. H. *Interpenetrating Polymer Networks and Related Materials*; Plenum Press: New York, 1981; pp 135−155.

MA071055P